

Scintillation detectors based on silicon microfluidic channels

This content has been downloaded from IOPscience. Please scroll down to see the full text.

2014 JINST 9 C01019

(<http://iopscience.iop.org/1748-0221/9/01/C01019>)

View [the table of contents for this issue](#), or go to the [journal homepage](#) for more

Download details:

IP Address: 131.94.16.10

This content was downloaded on 11/06/2015 at 21:09

Please note that [terms and conditions apply](#).

13th TOPICAL SEMINAR ON INNOVATIVE PARTICLE AND RADIATION DETECTORS
7–10 OCTOBER 2013
SIENA, ITALY

Scintillation detectors based on silicon microfluidic channels

**P. Maoddi,^{a,b,1} A. Mapelli,^a P. Bagiacchi,^c B. Gorini,^a M. Haguenaer,^a
G. Lehmann Miotto,^a R. Murillo Garcia,^a F. Safai Tehrani,^c S. Veneziano^c and
P. Renaud^b**

^aPhysics Department, European Organization for Nuclear Research (CERN),
Geneva, Switzerland

^bMicrosystems Laboratory, École Polytechnique Fédérale de Lausanne (EPFL),
Lausanne, Switzerland

^cSezione di Roma 1, Istituto Nazionale di Fisica Nucleare (INFN),
Rome, Italy

E-mail: pietro.maoddi@cern.ch

ABSTRACT: Microfluidic channels obtained by SU-8 photolithography and filled with liquid scintillators were recently demonstrated to be an interesting technology for the implementation of novel particle detectors. The main advantages of this approach are the intrinsic radiation resistance resulting from the simple microfluidic circulation of the active medium and the possibility to manufacture devices with high spatial resolution and low material budget using microfabrication techniques.

Here we explore a different technological implementation of this concept, reporting on scintillating detectors based on *silicon* microfluidic channels. A process for manufacturing microfluidic devices on silicon substrates, featuring microchannel arrays suitable for light guiding, was developed. Such process can be in principle combined with standard CMOS processing and lead to a tight integration with the readout photodetectors and electronics in the future. Several devices were manufactured, featuring microchannel geometries differing in depth, width and pitch. A preliminary characterization of the prototypes was performed by means of a photomultiplier tube coupled to the microchannel ends, in order to detect the scintillation light produced upon irradiation with beta particles from a ⁹⁰Sr source. The photoelectron spectra thus obtained were fitted with the expected output function in order to extract the light yield.

KEYWORDS: Manufacturing; Scintillators, scintillation and light emission processes (solid, gas and liquid scintillators)

¹Corresponding author.

Contents

1	Introduction	1
1.1	Microfluidic scintillation detectors	1
2	Fabrication of the microchannels	2
2.1	Etching of microchannels and fluidic openings in silicon	2
2.2	Surface smoothing and optical coating	3
2.3	Fluidic and optical packaging	5
3	Characterization of light yield	6
4	Conclusions	7

1 Introduction

Segmented detectors constituted by thin glass capillaries filled with liquid scintillators and coupled to CCDs are reported in literature [1, 2]. These devices operate similarly to detectors based on optical fibers, with light being generated in a scintillating core and guided to a photodetector, except in this case the core is constituted by the liquid scintillator while the glass serves as a cladding. The main advantage of this approach is the intrinsic radiation resistance resulting from the use of a liquid active medium: once its scintillation performance degrades under a certain threshold because of the radiation-induced damage, it is possible to empty the capillaries and refill them with fresh scintillator, without any complex intervention on the detector system. This is not the case with solid scintillators (fibers or tiles), in which replacing an active element also implies intervening on the corresponding mechanical and optical couplings.

However, this flexibility comes at the price of additional complexity, due to the need for liquid management in the system; moreover solutions based on the precise assembly of discrete objects into bundles, as is the case with both scintillating fibers and capillaries, are prone to introduce local defects affecting the spatial uniformity of the detector.

1.1 Microfluidic scintillation detectors

Microfluidic channels filled with a scintillating liquid were recently reported as a promising approach to overcome these difficulties [3]. In the reported case an array of microfluidic channels was patterned on a silicon substrate by SU-8 photolithography and coated with gold in order to provide a reflective surface. A serpentine geometry was used for the microchannels that allows to fill the whole array with liquid scintillator using a single fluidic inlet/outlet pair, hence in a much simpler way with respect to bundles of glass capillaries. Once filled with liquid scintillator, the microchannels define an array waveguides in which the scintillation light propagates along the

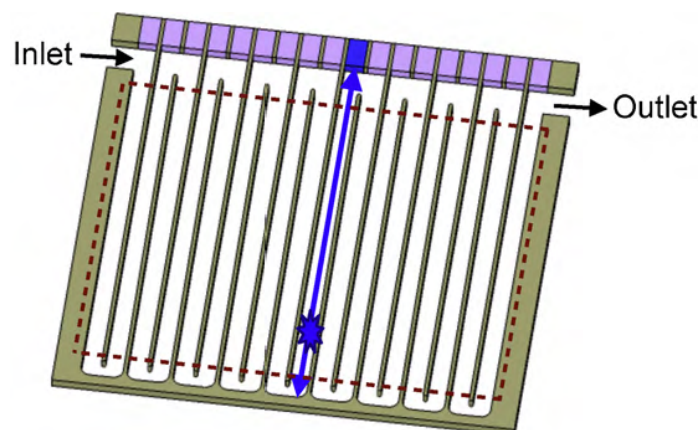


Figure 1: Operating principle of a microfluidic scintillation detector (reproduced from [3]). The microchannel array is filled with liquid scintillator by means of a single inlet/outlet pair. Upon passage of an ionizing particle through the detection zone (enclosed by the dashed line), light is generated by scintillation and guided along the microchannel to the corresponding element of the photodetector coupled to the side of the array.

microchannels by specular reflection off the gold layer, as depicted in figure 1. Prototype detectors based on microchannels with a thickness of up to $200\mu\text{m}$, and a pitch down to $60\mu\text{m}$ ($50\mu\text{m}$ wide channels separated by $10\mu\text{m}$ thick SU-8 walls) coupled to photomultiplier tubes were demonstrated, and their average light yield was measured to be of about 1.65 photoelectrons/MIP.

The microfluidic approach is of particular interest because it offers powerful methods to manipulate the liquid scintillators at small scales and relies on fabrication technologies directly derived from microsystems manufacturing, allowing for high geometric precision and repeatability. This paper reports on the development of scintillation detectors based on microfluidic channels fabricated in silicon, rather than polymers. Silicon is an extremely interesting material for this application, because of the many established techniques that exist for its microstructuring and most importantly because since it is a semiconductor it is possible in principle to integrate solid-state devices such as photodetectors and front-end electronics in the same substrate containing the microchannels, potentially leading to very compact detector systems.

2 Fabrication of the microchannels

2.1 Etching of microchannels and fluidic openings in silicon

An oxide layer was grown on the surface of a $380\mu\text{m}$ thick silicon wafer, then structured using standard photolithography and dry etching to reproduce the microchannel array pattern (figure 2a). A thick photoresist layer was spun on the wafer and patterned in such a way as to protect the whole surface except for some openings in correspondence of the fluidic inlets/outlets for the microchannels, then a standard deep reactive ion etching (DRIE) process was used to partially etch silicon (figure 2b). The photoresist was then removed, and the already patterned silicon oxide was used as a hard mask to etch deep microchannels in the silicon substrate (again by DRIE), while the previ-

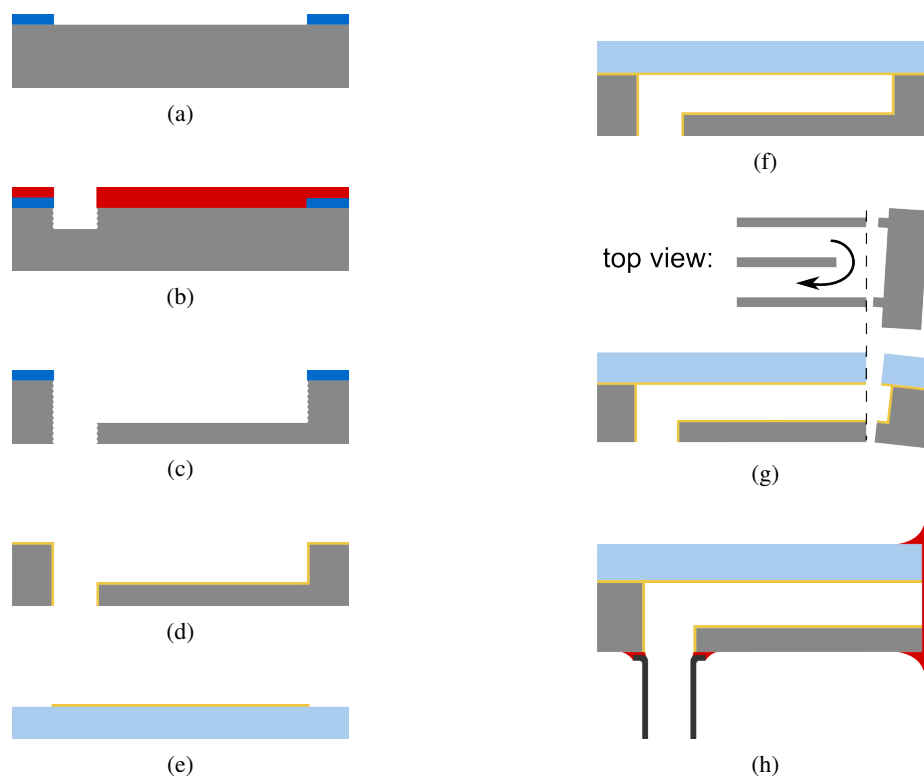


Figure 2: Schematic process flow for the fabrication of the microfluidic channels in silicon. (a) Dry etching of the microchannel pattern in silicon oxide, (b) partial silicon etching in correspondence of fluidic openings through a thick photoresist mask, (c) etching of the microchannels through the oxide hard mask and opening of the fluidic inlets/outlets with a single DRIE process, (d) smoothing of the silicon surface by SiO_2 growth/etching and metallization of the microchannels by Ti/Al sputtering, (e) patterning of Ti/Al reflective stripes on Pyrex cover wafer by lift-off, (f) anodic bonding of Pyrex and silicon wafer to close microchannels, (g) microchannel ends cut open during wafer dicing, in such a way that liquid circulation is still possible and (h) glueing of thin glass window and fluidic connectors.

ously partially etched areas reached the wafer backside, thus providing fluidic inlets/outlets for the microchannels (figure 2c).

2.2 Surface smoothing and optical coating

DRIE is a powerful anisotropic etching technique commonly used in MEMS manufacturing which relies on a cyclic sequence of fluorine-based plasmas that alternatively etch silicon and passivate the exposed lateral surfaces with a fluorocarbon film, allowing to obtain deep trenches with vertical sidewalls up to very high aspect ratios [4]. Although DRIE is an overall anisotropic process (i.e. etching preferably occurs along the out-of-plane direction in the substrate), a slight etching of the silicon in the in-plane direction occurs at each cycle before the passivation step, finally resulting in a typical undulation along the sidewalls, the so-called *scalloping* [5]. The sidewall of a microchannel exhibiting scalloping after the etching process is shown in figure 3a. This artifact

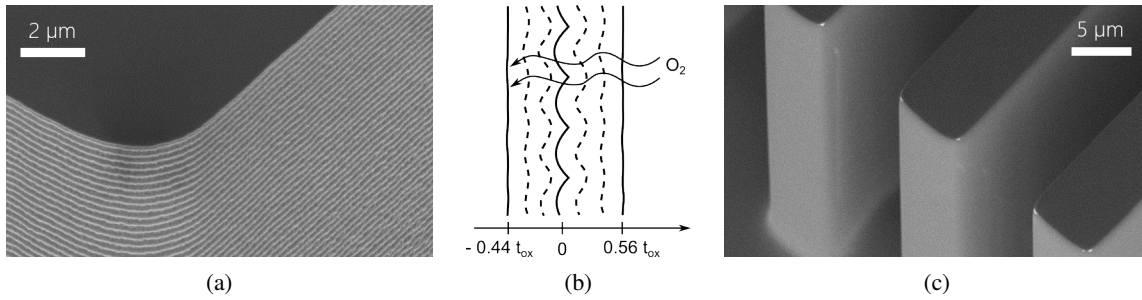


Figure 3: Smoothing of silicon microchannels. (a) SEM micrograph of silicon sidewalls after DRIE, exhibiting scalloping; (b) depiction of the evolution of the SiO_2 layer during wet oxidation of silicon. The initial silicon surface is located at 0. Silicon reacts with oxygen from the water vapor in the furnace environment, forming silicon oxide. The oxide layer distributes with approximately 44% of its thickness t_{ox} below and 56% over the original surface, because of the higher molar volume of SiO_2 with respect to Si. As the oxidation continues, oxygen must diffuse through the whole SiO_2 layer to reach the silicon surface underneath. The combination of these two effects causes the topography of the Si/SiO_2 interface (located at $-0.44t_{ox}$) to become flatter as the oxide thickness increases. (c) SEM micrograph showing smooth silicon after removing the oxide with hydrofluoric acid. In our case it was found that $t_{ox} = 3 \mu\text{m}$ is sufficient to eliminate scalloping with a 300 nm period.

is undesirable in applications involving optics such as ours, since the scalloping period (typically in the order of 100 to 400 nm) is comparable to the wavelength of the light emitted by the liquid scintillator (400 to 500 nm), resulting in sidewalls that behave as diffraction gratings or diffuse reflectors, thus degrading the light transport in microchannels.

In order to remove scalloping a smoothing process was developed, consisting in the growth of a $3 \mu\text{m}$ thick oxide layer on the etched silicon wafer by wet oxidation and its subsequent removal by buffered hydrofluoric acid (BHF). Because silicon oxidation is a process limited by the isotropic diffusion of the oxygen coming from the external environment, the shape of the Si/SiO_2 interface initially matches the scalloping undulation but tends to even out as the thickness of the oxide layer increases, as depicted in figure 3b. Hence, when the thick oxide layer is removed with BHF, the smooth silicon surface underneath corresponding to the former Si/SiO_2 interface is revealed, providing a surface suitable for light transport by specular reflections (figure 3c). Smooth microfluidic channels with several depths (ranging from 100 to $300 \mu\text{m}$) were fabricated with this method.

Since the reflectivity of a bare silicon surface is relatively low (reflectivity calculated at the emission peak of the liquid scintillator for an average angle: 37.1%), an optical coating is necessary to enhance the light transport in the etched microfluidic channels. Aluminium was chosen as a coating material because of its high reflectivity (calculated angular average: 89.3%), and ease of deposition. A 50 nm thick aluminium layer was deposited on the whole silicon wafer by conformal DC sputtering — over a 10 nm thick titanium adhesion layer — resulting in a mirror-like microchannel surface (figure 2d).

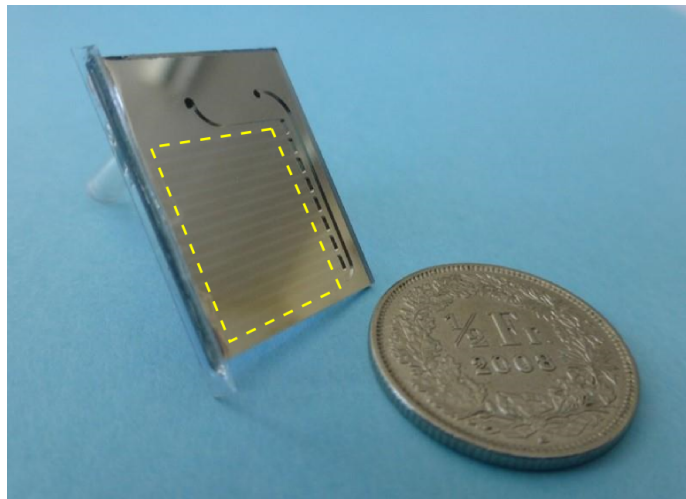


Figure 4: A $20 \times 15 \text{ mm}^2$ microfluidic chip, next to a coin for size comparison. The thin glass strip can be seen on the left side, while fluidic connectors for filling with the liquid scintillator are on the backside. The dashed line indicates the location of the $12 \times 12 \text{ mm}^2$ detection area.

2.3 Fluidic and optical packaging

In order to close the etched microfluidic channels, the same Ti/Al stack was deposited on a $525 \mu\text{m}$ thick Pyrex (CORNING 7740) wafer and patterned via a *lift-off* process to obtain reflective metal stripes slightly wider than the microchannels but with the same pitch (figure 2e); this geometry allows to align and put the wafers in contact in such a way that the metal stripes on the glass completely cover the microchannels,¹ while the bare glass surface can contact the top of the channel walls. This metal/Pyrex contact was exploited to solder the cover wafer and the wafer with the etched microchannels together using anodic bonding (350°C , 800V), thus yielding closed microfluidic channels with a mirror-like internal surface (figure 2f). A wafer-to-wafer alignment precision better than $5 \mu\text{m}$ could be consistently achieved using a SUSS MA6 aligner and SB6 bonder.

Since silicon is opaque in the wavelength range corresponding to the output of the liquid scintillator, it is necessary to provide a way out from the microchannels to the scintillation light. This was done by aligning the wafer dicing cut lines to the microchannels so that the latter are cut open on one side, but in such a way that it's possible to close them again without preventing the circulation of the liquid, as depicted in figure 2g. For this purpose, glass stripes (SCHOTT D263) with a thickness of $150 \mu\text{m}$ were glued to the side the chips, providing an optical interface to the microchannels. Connectors for tubing were glued in correspondence of the fluidic openings etched through silicon, providing a simple way to fill the microchannels with liquid scintillator (figure 2h).

The final prototype is pictured in figure 4, having a footprint of $20 \times 15 \text{ mm}^2$ with an active area of about $12 \times 12 \text{ mm}^2$. Versions with both 16 and 64 channels were produced, with a pitch of respectively 0.8 mm (500 or $700 \mu\text{m}$ wide channels) and 0.2 mm ($100 \mu\text{m}$ wide channels).

¹No aluminium was left in correspondence of the connections between microchannel ends opposite to the photodetector side, in order to minimize optical cross talk between neighbouring channels.

3 Characterization of light yield

The microfluidic chips were filled with a commercial liquid scintillator (EJ-305 from ELJEN TECHNOLOGY) and coupled to a photomultiplier tube (H3165-10 from HAMAMATSU). The devices were irradiated with electrons from a ^{90}Sr source (maximum energy: 2.3 MeV), using a plastic scintillating fiber (KURARAY SCSF-78, $0.5 \times 0.5 \text{ mm}^2$ square cross section) suitably aligned to the chips to trigger the readout on scintillation events from a single microchannel. An ADC (CAEN QDC V792) was used to digitize the charge signal from the PMT at each trigger event.

The average number of photoelectrons per MIP \bar{N}_{pe} produced by such a detector system can be expressed as:

$$\bar{N}_{pe} = \bar{N}_p \cdot \varepsilon_t \cdot \varepsilon_i \cdot \varepsilon_q \quad (3.1)$$

where \bar{N}_p is the average number of photons emitted in the scintillation event (dependent on the energy lost by the particle in the scintillator, so essentially on the depth of the microchannel), ε_t describes the light transport efficiency of the microchannel, i.e. the fraction of photons that is able to reach the microchannel/PMT interface, ε_i is the optical transmittance of such interface, and finally ε_q is the quantum efficiency of the PMT photocathode. In the case of a $190 \mu\text{m}$ deep, $700 \mu\text{m}$ wide microchannel, $\bar{N}_p \approx 307$ (calculated from the EJ-305 scintillator datasheet), $\varepsilon_t \approx 0.03$ (calculated via a Monte Carlo simulation of light propagation in the microchannel), $\varepsilon_i \approx 0.9$ (calculated using Fresnel equations) and $\varepsilon_q \approx 0.25$ (obtained from the H3165-10 PMT datasheet), yielding $\bar{N}_{pe} \approx 2$. This number slightly overestimates the actual value because it does not take into account losses arising from optical phenomena such as dispersion and not perfectly specular reflections on the microchannels inner surfaces as well as defects in the optical interface resulting from the glueing procedure.

The photoelectron spectra obtained from the experimental measurements were fitted with a function of the form:

$$f = f_{ped} + N \sum_n \mathcal{P}(n, \bar{N}_{pe}) \cdot \mathcal{N}(\mu_n, \sigma_n) \quad (3.2)$$

with

$$\mu_n = \mu_1 + nA \quad (3.3)$$

$$\sigma_n = \sigma_1 \sqrt{n} \quad (3.4)$$

(for $n > 1$)

where f_{ped} is the background signal measured using empty microfluidic channels and N is the number of scintillation events, so that the scintillation signal is given by the convolution of a Poisson distribution \mathcal{P} , describing the statistics of photoelectron production in the PMT photocathode, with a series of normal distributions \mathcal{N} , describing the electronics response to a given number of photoelectrons. Equations (3.3) and (3.4) describe the Gaussian $\mathcal{N}(\mu_n, \sigma_n)$ corresponding to n photoelectrons, in terms of the Gaussian $\mathcal{N}(\mu_1, \sigma_1)$ corresponding to a single photoelectron, related through the gain of the photomultiplier A , expressed in ADC counts per photoelectron.

The photoelectron spectrum from a $190 \mu\text{m}$ deep, $700 \mu\text{m}$ wide microchannel, fitted with eq. (3.2), yielding $\bar{N}_{pe} = 1.42$ is reported in figure 5. This light yield is consistent with the theoretical expectations from eq. (3.1) and the considerations reported previously and, albeit low, has to be put into perspective with the extremely small scintillator volume involved.

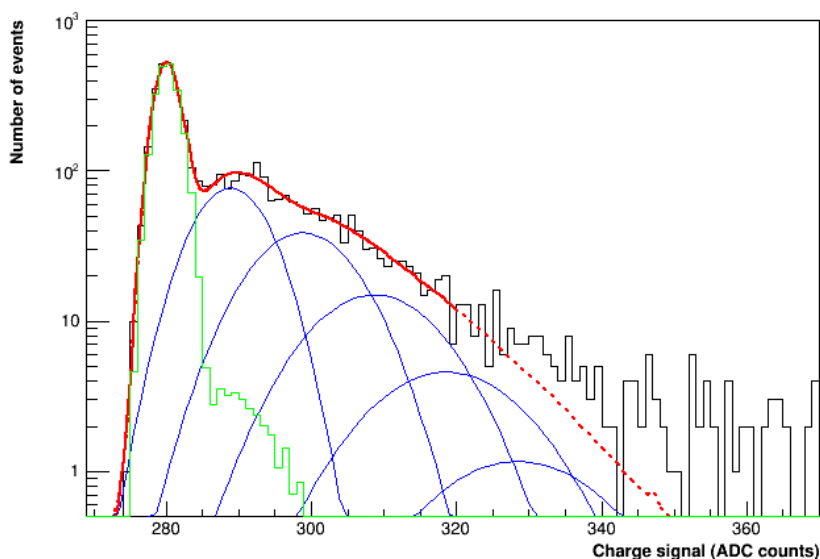


Figure 5: Photoelectron spectrum for a 190 μm deep, 700 μm wide microchannel (black histogram) fitted with eq. (3.2) (red line), yielding $\bar{N}_{pe} = 1.42$. The background signal measured using an empty microchannel (green histogram) and the Gaussians relative to the individual photoelectrons (blue lines) are shown as well.

4 Conclusions

A process relying on DRIE, oxidation and wafer bonding for manufacturing smooth, mirror-like microfluidic channels in silicon was developed. The light yield of the microchannels filled with liquid scintillator was measured with a radioactive source and a readout system based on photomultiplier tubes, resulting in an average of 1.42 photoelectrons per MIP, a result compatible with the theoretical expectations.

References

- [1] F. Ferroni and G. Martellotti, *Capillary fiber microvertex detectors*, *Nucl. Instrum. Meth. A* **368** (1995) 224.
- [2] A. Bay et al., *A high-resolution tracking hodoscope based on capillary layers filled with liquid scintillator*, *Nucl. Instrum. Meth. A* **457** (2001) 107.
- [3] A. Mapelli et al., *Scintillation particle detection based on microfluidics*, *Sensor. Actuat. A* **162** (2010) 272.
- [4] T. Pandhumsoporn et al., *High-etch-rate anisotropic deep silicon plasma etching for the fabrication of microsensors*, *Proc. SPIE* **2879** (1996) 94.
- [5] W.J. Park et al., *High aspect ratio via etching conditions for deep trench of silicon*, *Surf. Coat. Tech.* **171** (2002) 290.